AIAA/AAS Astrodynamics Specialist Conference and Exhibit
16 - 19 August 2004, Providence, Rhode Island

AIAA 2004-5217

Accommodating Rectangular Objects in Probability Calculations©

Salvatore Alfano *
Center for Space Standards and Innovation
7150 Campus Drive, Suite 260
Colorado Springs, CO 80920-6522

This work refines probability calculations for rectangular object shapes of unknown orientation and compares those results to their representations as spheres. Conjunction probability analysis for spherical objects exhibiting linear relative motion is accomplished by combining covariances and physical object dimensions at the point of closest approach. The resulting covariance ellipsoid and hardbody can then be projected onto the plane perpendicular to relative velocity. Collision potential is determined from the object's physical footprint on the projected, two-dimensional, probability density space. For rectangular objects, the attitude must be considered because the region of integration (footprint) changes. Ideally, the attitude of each object should be known to accurately assess this probability. In the absence of object attitude information, a footprint must be created that completely defines the region where the two objects might touch. This footprint can then be rotated to determine the orientation that produces the largest probability making it the most conservative estimate for the given conjunction conditions. For a rectangular object modeled as a circle, the representation is shown to be overly conservative, producing a larger probability than that of the rectangular shape.

Nomenclature

AR	=	aspect ratio of major-to-minor projected covariance ellipse axes
C_P_lo	=	correspondence of the low, relative probability value
dist	=	distance of closest approach
ht	=	individual object height
lt	=	individual object length
OBJ	=	combined object radius
P	=	two-dimensional probability
Pmax	=	maximum probability
r1	=	half-length of primary's largest dimension of projected rectangle
r1p	=	half-width dimension perpendicular to half-length r1
r2	=	half-length of secondary's largest dimension of projected rectangle
r2p	=	half-width dimension perpendicular to half-length r2
w	=	combined object width factor
wt	=	individual object width
x	=	major axis direction
xm	=	x component of projected miss distance
y	=	minor axis direction
ym	=	y component of projected miss distance
α	=	orientation angle of distance vector
σx	=	major axis standard deviation
σy	=	minor axis standard deviation
$\sigma y0$	=	zero order minor axis standard deviation approximation
θ	=	orientation angle of projected object

* Technical Program Manager, AGI/CSSI, 7150 Campus Drive, Suite 260, Colorado Springs, CO 80920-6522, salfano@agi.com, AIAA Associate Fellow.

Introduction

THERE is a growing body of work that addresses probability computations for neighboring space objects[1-9] and some literature that examines the associated accuracy requirements[10-11]. Typically, a determination is made when a secondary object transgresses a user-defined safety zone. The uncertainties associated with position are represented by three-dimensional gaussian probability densities. These densities take the form of covariance matrices and can be obtained from the owner-operators or independent surveillance sources such as the US Space Object Catalog (Special Perturbations). Typically, positions and covariances are propagated to the time of closet approach, relative motion is assumed linear, and the positional covariances are assumed constant and uncorrelated for the encounter.

Space object collision avoidance (COLA) is usually conducted with the objects modeled as spheres. The combined covariance size, shape, and orientation are coupled with physical object sizes to determine collision potential. At the point of closest approach, each object's positional uncertainty is combined and their radii summed. For linear relative motion, the resultant is projected onto a plane perpendicular to the relative velocity where the collision probability is calculated[9]. The projection reduces the probability formulation to a double integral that can be further simplified to a single integral through use of error functions.

This paper addresses the assumption that the objects are spherical. Satellite dimensions can be obtained by owner/operators or assessed through observation. The subsequent probability calculations can then be refined by using knowledge of the rectangular object shapes and their orientations. The non-circular footprint is integrated over the projected covariance. The attitude must be considered because it changes the region of integration (footprint). Ideally, the attitude of each object should be known to accurately assess probability. This paper shows how to create a footprint in the absence of object attitude information that completely defines the region where the two objects might touch. This footprint can then be rotated to determine the orientation that produces the largest (most conservative) probability for the encounter holding all other parameters fixed.

Formulation for probability with unknown orientation

A two-dimensional rectangle can be formed from the three-dimensional hard body object dimensions of height (ht), width (wd), and length (lt) such that all possible combinations of projection and attitude are completely contained. The all-encompassing rectangle has the dimensions shown in Fig. 1.

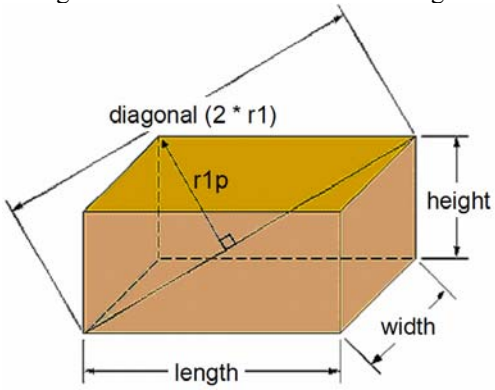

Figure 1. Primary object projection geometry.

The half-length (r1) of the primary rectangle is simply half the diagonal length

$$r1 = \frac{\sqrt{ht1^2 + wd1^2 + lt1^2}}{2} \tag{1}$$

The greatest half-width (r1p) perpendicular to r1 is

$$r1p = \sqrt{\max(ht1, wd1, lt1)^2 - \frac{\max(ht1, wd1, lt1)^4}{ht1^2 + wd1^2 + lt1^2}} \tag{2}$$

Similarly, the half-length (r2) of the secondary object's largest projected rectangle dimension is

$$r2 = \frac{\sqrt{ht2^2 + wd2^2 + lt2^2}}{2} \tag{3}$$

and the half-width (r2p) perpendicular to r2 is

$$r2p = \sqrt{\max(ht2, wd2, lt2)^2 - \frac{\max(ht2, wd2, lt2)^4}{ht2^2 + wd2^2 + lt2^2}} \tag{4}$$

The combined object radius (OBJ) is defined as

$$OBJ = r1 + r2 \tag{5}$$

and the width factor (w) is

$$w = \frac{\min(r1p + r2, r2p + r1)}{OBJ} \tag{6}$$

Figure 2 shows the overlay of the projected rectangle on the projected circle. The combined object must be coincidental to both spaces, meaning the shaded areas can be eliminated.

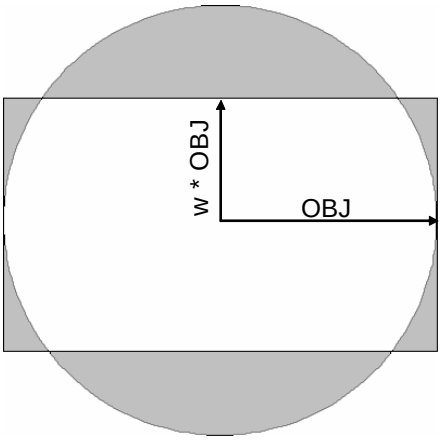

Figure 2. Superposition of projected rectangle and circle.

Because the orientation of the resulting projection is unknown, it must now be rotated through an angle θ measured from the covariance ellipse major axis. This is done to produce the largest probability for the given location (xm, ym) and associated standard deviations (σx, σy) in the projected covariance frame. As a function of θ the probability equation takes the form

$$P = \frac{OBJ^2}{2\cdot\pi\cdot\sigma y^2\cdot AR}\cdot\int_{-w}^{w}\int_{-\sqrt{1-y^2}}^{\sqrt{1-y^2}} \exp\left[\left(\frac{-1}{2}\right)\cdot\left[\left[\frac{[xm + (x\cdot\cos(\theta) + y\cdot\sin(\theta))\cdot OBJ]}{AR\cdot\sigma y}\right]^2 + \left[\frac{ym + (y\cdot\cos(\theta) - x\cdot\sin(\theta))\cdot OBJ}{\sigma y}\right]^2\right]\right] dx\, dy \tag{7}$$

where the major axis standard deviation (σx) has been replaced as the product of the aspect ratio AR and σy.

Formulation for maximum probability

This formulation determines the worst-case conjunction scenario by finding the combined Gaussian error probability density function that maximizes collision probability. A new angle (α) is introduced to define the orientation of the distance vector with respect to the covariance ellipse major axis. For a fixed miss distance (dist), object size (OBJ), and width factor (w), the projected covariance size and relative orientation are varied to produce the maximum probability while the covariance aspect ratio is held fixed. This is different from the previous section where the largest probability was found by varying θ while holding the covariance size (σy) and orientation (α) fixed. The angle α is illustrated in Fig. 3 along with the orientation angle of the projected object (θ).

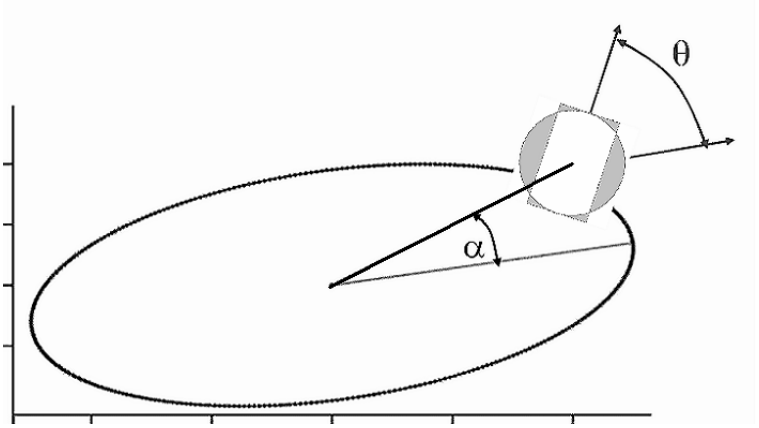

Figure 3. Relationship of angles α and θ to major axis.

The probability equation as a function of α and θ becomes

$$P = \frac{OBJ^2}{2\cdot\pi\cdot\sigma y^2\cdot AR}\cdot\int_{-w}^{w}\int_{-\sqrt{1-y^2}}^{\sqrt{1-y^2}} \exp\left[\left(\frac{-1}{2}\right)\cdot\left[\left[\frac{[dist\cdot\cos(\alpha)+(x\cdot\cos(\theta)+y\cdot\sin(\theta))\cdot OBJ]}{AR\cdot\sigma y}\right]^2+\left[\frac{dist\cdot\sin(\alpha)+(y\cdot\cos(\theta)-x\cdot\sin(\theta))\cdot OBJ}{\sigma y}\right]^2\right]\right] dx\,dy \tag{8}$$

Figure 4 shows a parametric representation of probability with respect to the two angles for all aspect ratios greater than one and width factors less than one.

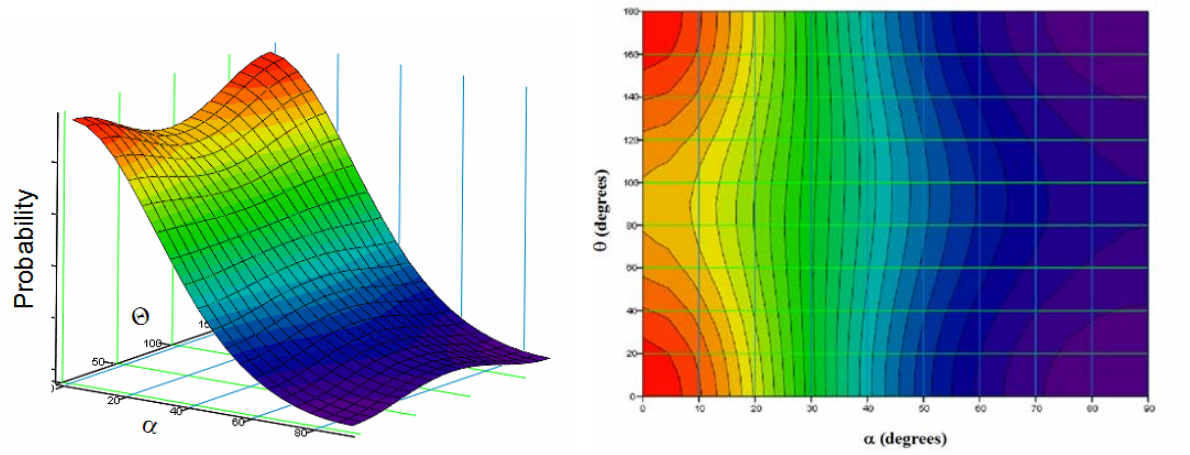

Figure 4. Probability with respect to angles α and θ.

As deduced from Fig. 4, the maximum probability appears to occur when the relative position vector is aligned with the major axis of the combined covariance ellipse (α equals zero) coincident with the object's probability mass symmetrically distributed about the major axis (θ equals zero). It can readily be shown that under these conditions, the first derivative with respect to each angle is zero and their second derivatives are negative. The maximum probability for a given covariance size (σy) and shape (AR) is therefore represented as

$$Pmax = \frac{OBJ^2}{2\cdot\pi\cdot\sigma y^2\cdot AR}\cdot\int_{-w}^{w}\int_{-\sqrt{1-y^2}}^{\sqrt{1-y^2}} \exp\left[\left(\frac{-1}{2}\right)\cdot\left[\left[\frac{(dist + x\cdot OBJ)}{AR\cdot\sigma y}\right]^2 + \left(\frac{y\cdot OBJ}{\sigma y}\right)^2\right]\right] dx\, dy \tag{9}$$

With θ equaling zero to optimize the object orientation and α equaling zero to optimize the relative distance direction, the final step determines the size of the projected covariance that maximizes Eq. (8). The derivative of Eq. (9) is taken with respect to σy and the resulting exponential function in the integrand approximated to zeroth order. The resulting double integral is set equal to zero to determine the minor axis standard deviation σy that maximizes the probability. This zero-order approximation ($\sigma y0$) becomes

$$\sigma y0 = \sqrt{\frac{-OBJ^2}{24}\cdot\frac{\left[\left(-2 + 6\cdot AR^2\right)\cdot w\cdot\left(\sqrt{1 - w^2}\right)^3 + \left[-3\cdot AR^2 - 3 - 12\cdot\left(\frac{dist}{OBJ}\right)^2\right]\cdot w\cdot\sqrt{1 - w^2} + \left[-3\cdot AR^2 - 3 - 12\cdot\left(\frac{dist}{OBJ}\right)^2\right]\cdot\operatorname{asin}(w)\right]}{AR^2\cdot\left(w\cdot\sqrt{1 - w^2} + \operatorname{asin}(w)\right)}} \tag{10}$$

The value of the above expression can be used in Eq. (9) to begin iterating on σy to find the maximum probability within the bounds of user tolerance.

If the combined object footprint contains the covariance ellipsoid center (dist < OBJ), the maximum probability approaches one as the minor axis' standard deviation nears zero. This is the limiting case and must be independently addressed. The method described in this section only applies when the combined object does not encompass the covariance center (dist $\geq$ OBJ). Given the combined object radius, width factor, and distance from center, the minor axis size can be determined by maximizing the above probability expression with respect to σy. Once determined, the worst-case collision probability is calculated.

Numerical Testing

Approximately 500,000 test cases were used to evaluate the preceding probability expressions. These cases had all parameters normalized to a minor axis standard deviation of 1. The object size varied from 10^{-3} to 10^{+3}, the miss distance varied from 10^{-4} to 10^{+3} with position ranging from 0° to 90° relative to the major axis (α), and the aspect ratio varied from 1 to 50. Additionally, the object's orientation angle (θ) was varied from 0° to 180° relative to the major axis with the width factor ranging from 0.01 to 0.99. To understand the benefits of treating objects as rectangles, all results are given as a percentage of the probability for spherical objects. In the representative plots that follow, a solid red line with diamonds indicates the mean relative probability, a dashed green line with x symbols represents the maximum relative probability, a blue dotted line with circles represents the minimum relative probability, and a black dash-dotted line with plus signs represents the mean approximation. All computations were done using MATHCAD 11 set to the highest tolerance that would still allow convergence of the integrals. For these cases the tolerance was set to 10^{-11}.

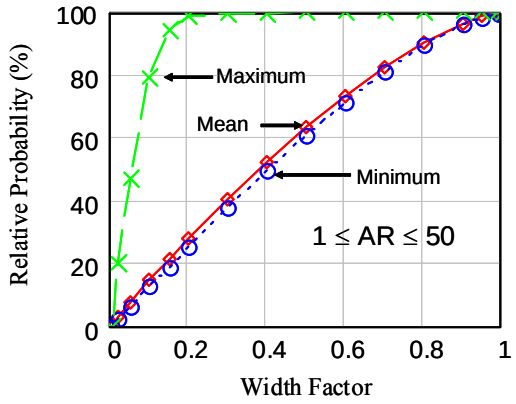

Figure 5. Relative Probability (OBJ < dist)

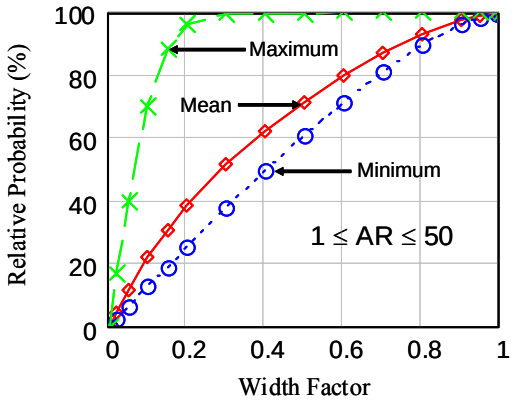

Figure 6. Relative Probability (OBJ ≥ dist)

The above figures show the characteristic behavior of the probability function with respect to the width factor. The correspondence of mean value is not one-to-one with the width factor. When the combined object radius is less than the relative distance, the mean and minimum values are somewhat close in value as reflected in Fig. 5. The correspondence of the low, relative probability values (C_P_lo) can be approximated by comparing the footprint area of the projected rectangular object to that of the circular one through the following equation.

$$C\_P\_lo \approx \frac{2\cdot\left(w\cdot\sqrt{1-w^2}+\operatorname{asin}(w)\right)}{\pi} \tag{11}$$

The above equation is a simple indicator of what improvement should be expected (on average) when using a rectangular shape instead of a circular one. The comparisons of the approximation to mean and low, relative probability values are shown in the following figure.

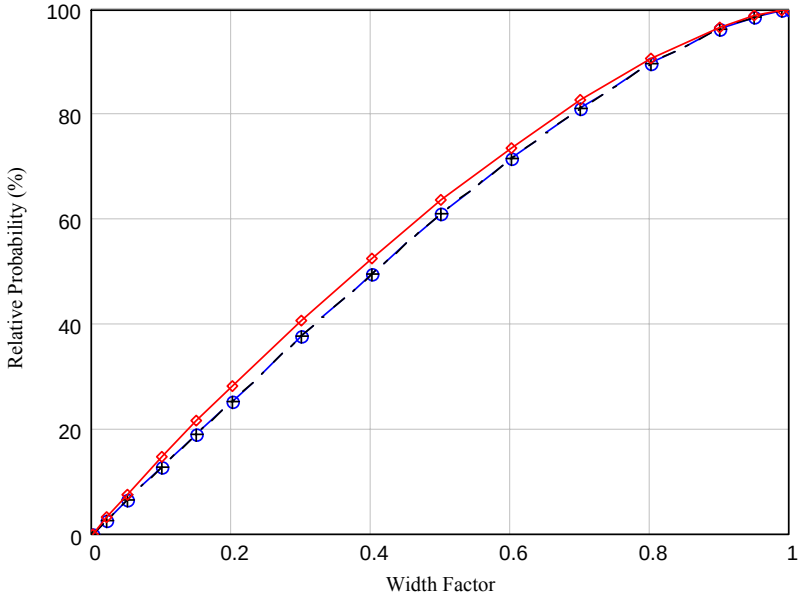

Figure 7. Relative Probability Approximation Comparison (OBJ < dist)

The maximum probability expression was evaluated in a similar manner. The object radius was smaller than or equal to the miss distance and no limit was set on the standard deviation. The object's orientation angle (θ) and relative distance angle (α) were fixed at zero with all other parameters varied as previously mentioned. As before, all results are given as a percentage of the maximum probability for spherical objects. The legend description for the following figure also remains the same as does the MATHCAD 11 tolerance.

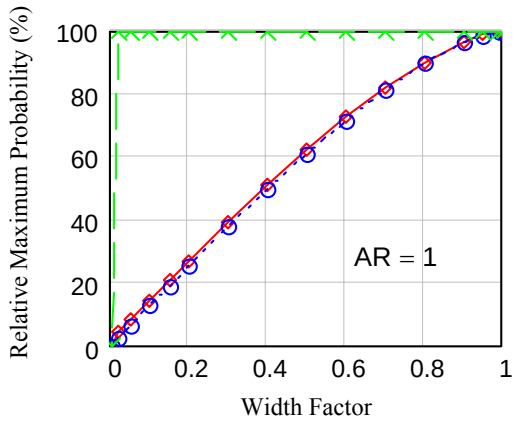

Figure 8. Relative Max Probability (AR=1)

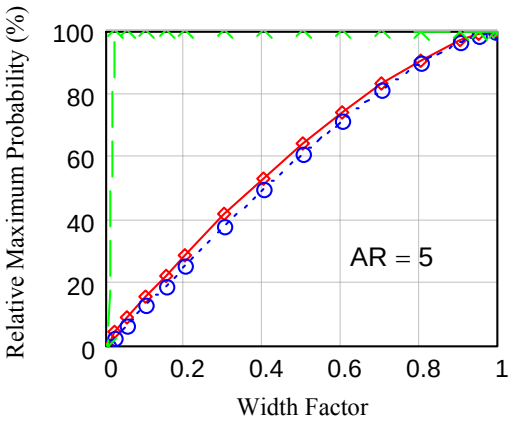

Figure 9. Relative Max Probability (AR=5)

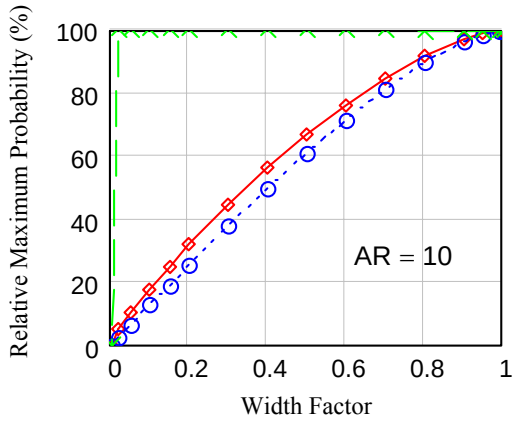

Figure 10. Relative Max Probability (AR=10)

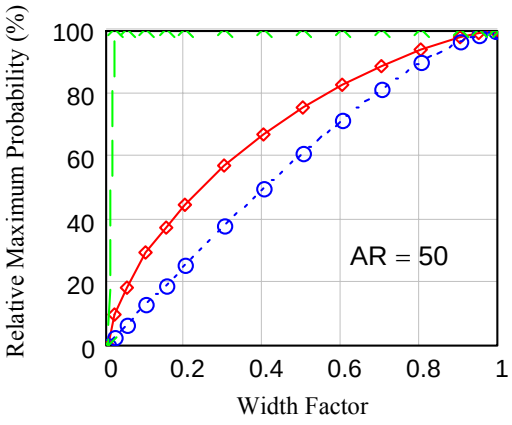

Figure 11. Relative Max Probability (AR=50)

Figures 8-11 show the characteristic behavior of the maximum probability function with respect to the width factor and aspect ratio. The standard deviation that produces the maximum probability decreases as the width factor decreases. If the standard deviation is unconstrained and the object radius approaches the miss distance in value, the probability density becomes more concentrated near the origin. This has a twofold effect as seen in the figures. The most obvious effect is that the greatest relative maximum probability (dashed green line with x symbols) approaches 100% rapidly. The second effect is that the mean relative values (solid red line with diamonds) also tend to be greater as the aspect ratio grows.

It is beneficial to get a sense of the width factor's variability. Every day that new NORAD two-line element sets are publicly released, a maximum conjunction probability report is generated and posted as a free advisory service at the website http://celestrak.com/SOCRATES/. The June 29, 2004, data was used to determine all object pairings of primaries (2,627) with secondaries (8,411) within 10 kilometers for a seven day span. The width factor for each of the resulting 26,752 pairs was then computed and binned to produce the following histogram.

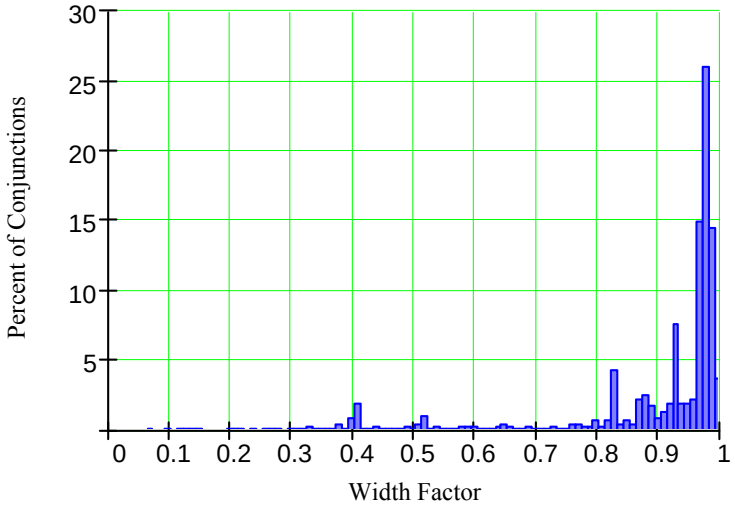

Figure 12. Width Factor Histogram

Conclusion

Conservative expressions were derived for the conjunction probabilities of rectangular objects in the absence of attitude information. An approximation to mean probability relative to that of a circular object was also given. A width factor histogram for a single run of Satellite Orbital Conjunction Reports Assessing Threatening Encounters in Space (SOCRATES) was provided to give the reader a snapshot of variability.

References

[1]Foster J. L., and Estes, H. S., "A Parametric Analysis of Orbital Debris Collision Probability and Maneuver Rate for Space Vehicles," NASA JSC 25898, August 1992.

[2]Khutorovsky, Z. N., Boikov, V., and Kamnesky, S. Y., "Direct Method for the Analysis of Collision Probability of Artificial Space Objects in LEO: Techniques, Results, and Applications," Proceedings of the First European Conference on Space Debris, ESA SD-01, pp. 491-508, 1993.

[3]Carlton-Wippern, K. C., "Analysis of Satellite Collision Probabilities Due to Trajectory and Uncertainties in the Position/Momentum Vectors," *Journal of Space Power*, Vol. 12, No. 4, 1993.

[4]Chan, K. F., "Collision Probability Analyses for Earth Orbiting Satellites," Advances in the Astronautical Sciences, Vol. 96, pp. 1033-1048, 1997.

[5]Berend, N., "Estimation of the Probability of Collision Between Two Catalogued Orbiting Objects," Advances in Space Research, Vol. 23, No. 1, pp. 243-247, 1999.

[6]Oltrogge, D., and Gist, R., "Collision Vision Situational Awareness for Safe and Reliable Space Operations," 50th International Astronautical Congress, 4-8 Oct 1999/Amsterdam, The Netherlands, IAA-99-IAA.6.6.07.

[7]Akella, M. R., and Alfriend, K. T., "Probability of Collision Between Space Objects," Journal of Guidance, Control, and Dynamics, Vol. 23, No. 5, September-October 2000, pp. 769-772.

[8]Chan, K. F., "Analytical Expressions for Computing Spacecraft Collision Probabilities," AAS Paper No. 01-119, AAS/AIAA Space Flight Mechanics Meeting, Santa Barbara, California, 11-15 February, 2001.

[9]Patera, R. P., "General Method for Calculating Satellite Collision Probability," *AIAA Journal of Guidance, Control, and Dynamics*, Volume 24, Number 4, July-August 2001, pp. 716-722.

[10]Gottlieb, R. G., Sponaugle, S. J., and Gaylor, D. E., "Orbit Determination Accuracy Requirements for Collision Avoidance," AAS/AIAA Space Flight Mechanics Meeting, February 11-15, 2001, Santa Barbara, California, AAS 01-181.

[11]Alfano, S., "Relating Position Uncertainty to Maximum Conjunction Probability," AAS Paper No. 03-548, AAS/AIAA Astrodynamics Specialist Conference, Big Sky, Montana, 3-7 August, 2003.